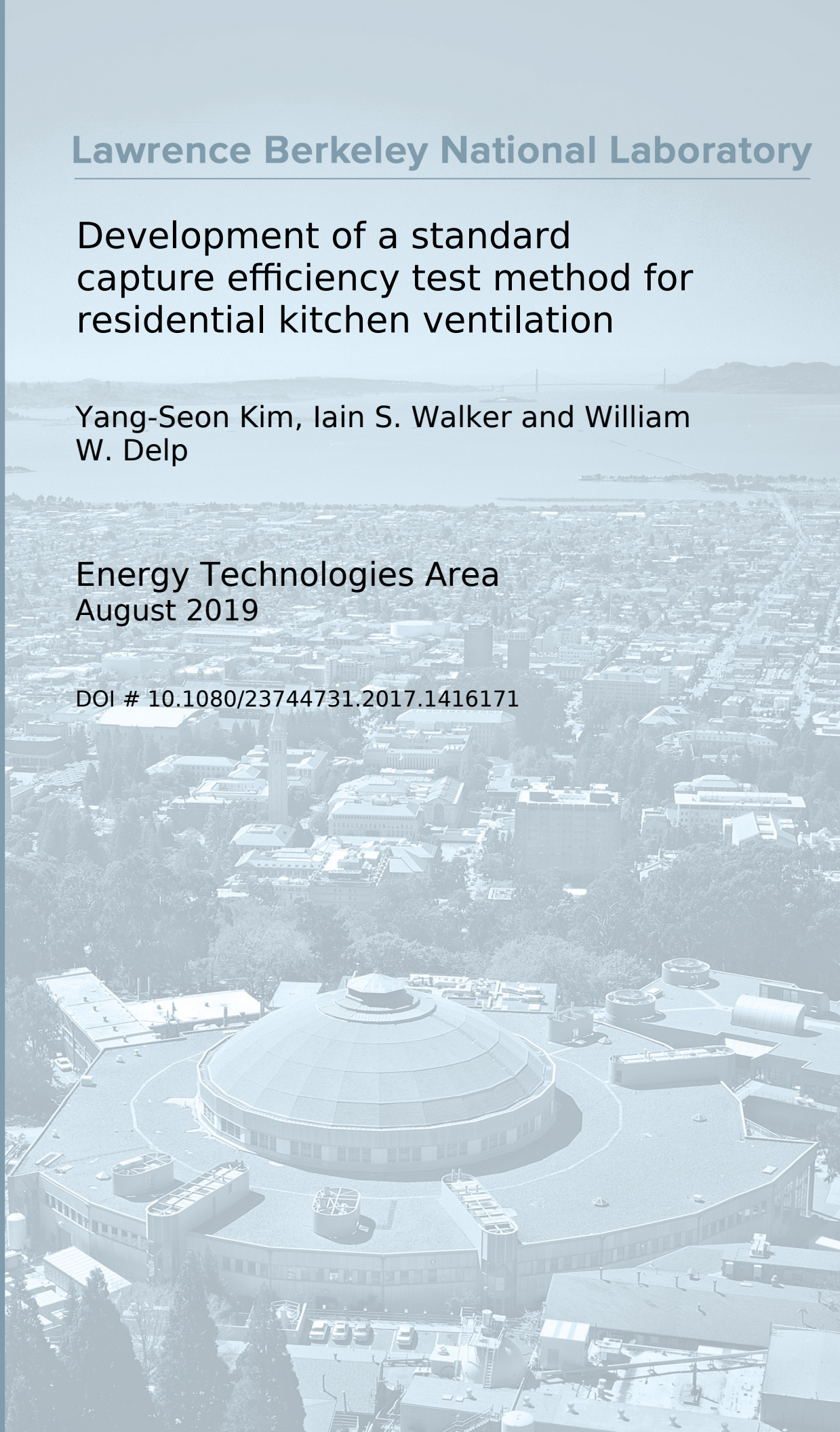

BERKELEY LAB

Lawrence Berkeley National Laboratory

Development of a standard capture efficiency test method for residential kitchen ventilation

Yang-Seon Kim, Iain S. Walker and William W. Delp

Energy Technologies Area
August 2019

DOI # 10.1080/23744731.2017.1416171

ABSTRACT

Cooking activities are a major source of indoor air pollutants. To control pollutants generated from cooking activities, a range hood is commonly used in residential kitchens. Several building codes require that a range hood be installed in new homes to control pollutants from cooking, and the required airflow rates for range hoods are specified by indoor air quality (IAQ) standards. However, air flow alone does not tell us how much of the cooking pollutants are exhausted by the range hood. A better metric to evaluate range hood IAQ performance is capture efficiency (CE)—the fraction of contaminants emitted during cooking that are exhausted directly to the outside via the range hood. This paper summarizes the development of a range hood CE test method for use in laboratory testing and equipment rating.

INTRODUCTION

The objective of this paper is to summarize the laboratory test method that was developed to determine CE for residential wall-mounted range hoods, and the results of applying these test methods to sample range hoods. It includes the strategies and results from initial and intermediate versions of the test method as it was developed, in addition to the final test method.

This new test method is intended to be used as an ASTM standardized test method to evaluate residential range hoods. Its development included input from the ASTM working group responsible for writing the ASTM test method. This group includes range hood manufacturers, researchers, and potential users of the test method. The ASTM test method is nearing publication at the time of writing (August 2017).

Cooking activities are a major source of pollutants of concern for health, such as sub-2.5 micron particulate matter ($PM_{2.5}$), ultrafine particles (less than 0.1 micron diameter), nitrogen dioxide (NO_2), carbon monoxide (CO), and formaldehyde (CH_2O). Cooking also produces moisture and odors that need to be controlled for acceptable indoor air quality (IAQ). In addition, Several studies have found that combustion products from the natural gas used for cooking can cause a variety of respiratory health problems, such as asthma and allergies (Huang et al. 2011; Siegmann and Sattler 1996; See et al. 2005) and ultrafine particles, which can cause respiratory problems, are generated from electric heating elements (Dennekamp et al. 2001; Wallace et al. 2017; Wallace et al. 2014; Buonanno et al. 2009). There are two types of residential range hoods: recirculating and venting. Recirculating range hoods return the air directly to the kitchen and remove very little contamination; typically they only have a grease filter. Venting range hoods exhaust kitchen contaminants directly to the outside and are seen as an effective method of source control for cooking-related contaminants.

To control pollutants generated from cooking activities, a range hood mounted over the cooktop is commonly used in residential buildings. Several studies (Logue et al. 2013; Rim et al. 2012; Singer et al. 2012) have shown reductions in cooking-related indoor air pollutants due to range hood use. In simulation studies, range hoods have been shown to reduce the frequencies of pollutant concentrations that exceed the health-based pollutant standards in homes by factors of 2 to 3 (Logue et

al. 2013). Laboratory studies have demonstrated particle concentration reductions from 94% to 31% for front heating elements and from 98% to 54% for back heating elements (Rim et al. 2012).

The rate of plume spread and the velocities in the plume are likely to affect the capture efficiency of a range hood. The physical size of the plume will determine how much of the plume strikes the underside of a range hood or misses the range hood and escapes into the room. The plume velocities interact with the induced velocities from the range hood operation. The lower the plume velocities relative to the induced range hood air velocities, the greater the likelihood that the plume is captured. To investigate the effect of exhaust systems on reducing the pollutant exposure from cooking activities, previous studies (Kosonen et al. 2006 (a); Kosonen et al. 2006 (b); Li et al. 1996; Honda et al. 2012) investigated the thermal plume dynamics from heat sources. These studies showed that fully developed plumes have a Gaussian velocity profile and the following characteristics. The plume formation from the heat source is dominated by temperature, the diameter of heat source, and initial velocity. In the case of cooking, the initial velocities are zero, but many other plume situations, such as industrial stacks, have significant initial plume velocity. The plume diameter grows linearly with height: the axial velocity (v) decreases with height (to the -1/3 power); and the plume temperature (T) decreases rapidly with height to the -5/3 power, due to entrainment of the surrounding air.

While these relationships provide some guidance, the plume does not have enough space to become fully developed. The buoyant plume is sensitive to outside disturbances such as other air flows in the room (from infiltration, heating and cooling forced air systems, open windows, etc.), proximity of impervious surfaces (walls, floor, ceiling, cabinets) and the flow pattern established in the room by the range hood. Therefore, it is difficult to calculate the plume using a purely analytical approach and experimental data are needed to better understand the plume dynamics. Several studies have measured the velocities and temperature above kitchen appliances such as gas or electric cooktops and showed that the power intensity of the heat source (power input per source burner—or power input for a given burner physical size) has a significant effect on the plume characteristic (Kosonen et al. 2006a). The plumes are narrower and the spreading angle is smaller than for the fully developed plume theory, in both idle mode (i.e., active heat source but without cooking) and cooking mode (Kosonen et al. 2006a, 2006b). Experiments with boiling water (with the same input power) showed that plume temperatures and velocities also depended on the pot size (Honda et al. 2012).

Several building codes require that a range hood be installed in new homes to control pollutants from cooking, and the required airflow rates for range hoods are specified by indoor air quality standards. For example, ASHRAE Standard 62.2-2016 requires a minimum exhaust airflow rate of 100 cubic feet per minute (CFM) (50 liters per second, L/s), together with a sound rating of 3 sone or less (ASHRAE 2016). The ASHRAE standard uses air flow as a metric of interest when considering kitchen ventilation because air flow measurements are readily available and have been used as a metric of performance for many years. The ASHRAE standard limits the sound level because of concerns that noisy kitchen exhaust devices are less likely to be used by occupants, particularly in modern homes where the kitchen is

not an isolated room. Manufacturers provide air flow rates in product specifications, and the Home Ventilating Institute (HVI) has a directory of certified air flow rates for range hoods (HVI 2015)—with measured flows at standardized conditions.

Existing test methods for commercial kitchen hoods (ASTM 2009) use flow visualization techniques to check whether or not the entire plume is captured by the hood. The flow visualization techniques include schlieren visualization and shadowgraphs, or theatrical fog. The hood air flow rate is varied until full capture and contaminant of the thermal/effluent plume is achieved. Guidance is provided for evaluating capture, such as: “Any observed leak moving beyond 3 inches (7.6 cm) from the hood face will be construed to have escaped from the hood, even if it may appear to be drawn back into the hood (ASTM 2009).”

However, for residential hoods, our goal is not necessarily full plume capture, primarily because there is much less cooking in residential buildings and using the physically large and high airflow (requiring dedicated makeup air) equipment found in commercial kitchens would be overly burdensome. Therefore, a test method is required that will work without full capture. Because the flow visualization techniques are only applicable to detecting full capture and do not provide quantitative estimates of partial capture, these existing commercial hood test methods are not appropriate.

Other metrics have been used to test kitchen exhaust hood performance. For example, Rim at al. (2012) used the ratio of integrated particle concentration differences between range hood on and off tests to calculate the whole house particle reduction effectiveness, and the European standard for range hood performance (IEC 2005) includes fan performance, grease absorption, and odor extraction. Kuehn et al. (1989) performed laboratory experiments on residential kitchen exhaust fans that used flow visualization with sound measurements. These previous studies showed that air flow alone is insufficient to determine how much of the cooking pollutants are exhausted by the range hood. Some other researchers (Li et al. 1996 and Gao et al. 2013) used simulations to estimate range hood performance that are appropriate for range hood design, but are not practical for a standardized range hood efficiency test.

The most appropriate performance metric for removal of cooking pollutants is *capture efficiency* (CE), defined as the fraction of pollutants emitted during cooking that are exhausted directly to the outside. A CE of 100% means that all of the cooking pollutants are exhaust directly to the outside, and a CE of zero means no pollutants are directly exhausted, allowing all of them to mix with indoor air.

Two previous Lawrence Berkeley National Laboratory (LBNL) studies conducted tests for residential kitchen hood CE in the laboratory and in the field. Both CE tests were conducted with pots of boiling water on a gas cooktop. Singer et al. (2012) conducted on-site performance testing for 15 different range hoods, which were already installed and used in homes. The results of these tests are shown in Figure 1, where the types of range hoods are identified by a letter/number identifier. Four different types of range hoods were tested and categorized by their geometry —(1) downdraft (D1, D2), (2) flat bottom (F1, F2, F3, F4, F5), (3) hybrid (capture volume above grease screens) (H1, H2), and (4) open (bowl) (B1, B2, B3, B4, B5). The

source locations were also varied: front burenrs only, back burners only, front and back burners simultaneously, and the oven.

The CE was calculated using measurements of airflow (Q (m^3/minute)), the CO_2 concentration differences between the room and the range hood exhaust (ΔCO_2 (ml)/m^3), and the CO_2 emission rate (S (ml/minute)), as shown in Equation 1 below (Delp et al. 2012):

$$CE = \frac{Q \bullet \Delta CO_2}{S} \qquad (1)$$

The source of the CO_2 was the natural gas burners on the cooktop. The CO_2 emission rate was calculated from stoichiometry, assuming complete combustion and the measured gas fuel flow rate (with an assumed molar fraction of carbon in the fuel). Note that using the gas burner to seed the plume with tracer only seeds an annulus of plume around the pot such that the CE is of the burner-related pollutant part of the plume and does not include the CE from the cooking itself because the core part of the plume is not seeded. This study found a large range of CE. Downdraft devices were generally poor performers, primarily because the exhaust air is level with or below the heating elements/cooking and resulting hot plume. For wall-mount devices, their performance depended largely on which heating elements were used and the air flow rate. The lowest capture efficiency was for flat-bottomed hoods (particularly microwave range hood combinations) when front burners were used. This depended on hood geometry—the more of the front heating elements that are covered by the hood, the better the plume is captured for these heating elements.Higher airflow generally led to higher capture efficiency, and the CE was much higher for the back heating elements near the wall.

Delp and Singer (2012) conducted laboratory tests for seven different range hoods: Basic, low cost (L1); Basic, quieter (B1); Compliant with requirements of the ASHRAE 62.2. (A1); ENERGY STAR rated (E1); ENERGY STAR rated (E2); Microwave range hood (M1); and Premium range hood (P1). These laboratory tests used the same approach—using CO_2 from gas burners as the tracer to seed the plume. This laboratory study showed very similar results to the field study, with CE values ranging from 17%–100% with a strong dependency on air flow and burner/heating element/range hood geometries.

Figures 1 (a) and (b) show the summary results from these previous studies. Figure 1 (a) shows the field results (Singer et al. 2012 and (b) shows the laboratory results (Delp and Singer 2012). Overall, these results show that the CE range is large even at a single air flow, which implies that CE would be a much better performance specification than air flow for range hood IAQ performance. To do this in a uniform and consistent way requires development of a test method, and the rest of this paper discusses that effort.

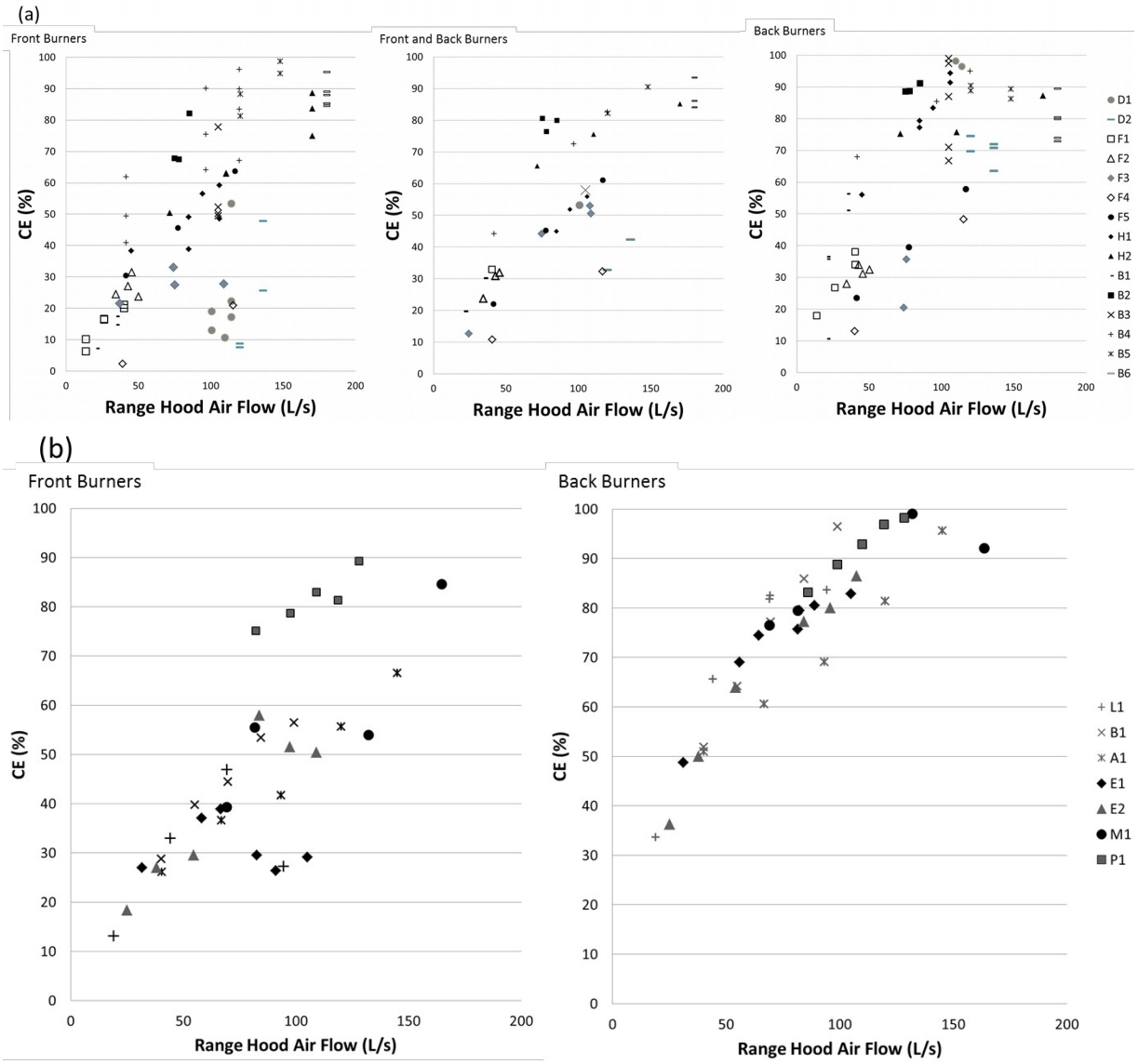

Figure 1. Summary CE results from previous LBNL studies. Note that the range hood codes are consistent with the references (Singer et al. 2012and Delp and Singer 2012).

Other studies have estimated range hood capture efficiency for pollutants other than CO_2. Farnsworth et al. (1989) conducted laboratory tests on a gas cooktop with open pots filled with water with several different range venting options as part of the development of a fully vented gas range. Nitrogen oxides (NO_x) and water vapor were used to calculate capture efficiency. The source of the NO_x was the cooktop gas burners. The results of the NO_x testing showed that higher air flow led to higher capture efficiency. For a canopy hood operating at 94 L/s, the capture efficiency was much higher when two rear burners were used (91%) than when two front burners were used (62%). With all four burners operating the NO_x-based capture efficiency was 70%. The water vapor capture showed similar results; the two rear burners had much better capture efficiency (90%) than the two front burners (42%) and all four burners (63%). This study also found other interesting results: the gas downdraft

system showed an almost 100% NO_x capture efficiency when using the high-height (229 millimeter [mm]) pot or the low-height (127 mm) pot for water boiling; however, it was relatively ineffective for water vapor capture; the high-height pot had much lower capture efficiency (11%–51%) than the low-height pot (43%–86%). This make sense because the downdraft system only captures air near the burners – the source of the NO_x. Lunden et al. (2015) compared capture efficiency using CO_2 and cooking generated particles. Capture efficiency for particles were similar to CO_2-based capture efficiency for pan frying on back burners. However, for stir-frying on front burners, CO_2-based capture efficiency (with 109–138 L/s fan flow; 54%–72% of CE) was higher than particle-based capture efficiency (with 109–138 L/s fan flow; 16%–70% of CE). The differences between CO_2 and particle-based capture efficiency changed depending on the particular range hood being tested.

These previous studies also identified some key issues that were considered in the development of the CE test method:

- Requiring measurements of airflow rates introduces additional uncertainty into CE calculations.
- Using measurement of the gas fuel flow rates and assumed carbon content of the fuel to calculate the CO_2 emission rate can introduce additional uncertainty into the CE calculations.
- Pot dimensions need to be strictly defined for consistency among the tests. Pot size changes the initial plume size and shape as it flows around the pot, which can change the CE.
- Testing should consider both front and back heating elements due the differences in CE for their emissions. After much discussion with the American Society for Testing and Materials (ASTM) Task Group and laboratory testing of several combinations of active heating elements (two fronts, two back, and one back and one front diagonally opposite each other) it was decided that two front heating elements should be used because this present the greatest challenge for plume capture. This configuration shows the greatest variability from range hood to range hood and are the locations used most often when cooking.
- The range hood mounting height and air flow rate during testing must considered and at least recorded for testing.

To address these issues, the test method was developed to have the following attributes:

- Testing is done at steady state. Although it is possible to use non-steady-state tracer gas measurements, the calculations are more complex and introduce additional test uncertainty.
- Calculate CE from concentration measurements in the room, the range hood exhaust, and at the inlet to the test chamber. This obviates the need to also measure air flows and air densities with their associated uncertainties.
- Instead of a using a gas burner as a tracer gas source, deliberately emit a tracer over the heated surface—thus seeding the whole plume and not just the annulus associated with the gas burner flow around the pot edges.
- Use a standardized cooking event. Through consultation with the ASTM Task Group a moderate cooking event was decided upon. It is between the extremes of high heat/large pot (e.g., stir frying) and low heat/small pot (e.g., simmering a sauce). It was decided that heating elements be operated at

1,000 watts (W) and at a temperature of 200°C ±10°C (390°F ±18°F). For safety and ease of measurement it was decided that electric heating elements should be used.

- Use a standardized tracer gas emitter. This ensures that when the test method is performed in different test laboratories there is consistency of tracer gas emission. Tracer emitters of specific dimensions were developed that can be easily replicated. The tracer is emitted at multiple locations over the whole plume source. This includes the flow around the bottom of the pot from heating elements, as well as from above the pot for cooking contaminants. The emitter was designed to have a gap between two plates with hot air that escapes around the edges. Although imperfect, this is an attempt to mimic somewhat the hot jet of combusting gases from a gas burner.
- No pot with boiling water is used. Boiling water removes about 40%–65% of the heating energy from the plume, and for the plume to be consistent from test to test we would need to carefully control the boiling—which may be hard to accomplish in a standardized, replicable way (Kosonen et al. 2006b). We want to be able to control both the power put into the plume and the surface temperature of the emitter— which a pot of boiling water would also complicate. Lastly, safety and test equipment calibration concerns arise if humidity is high in the test chamber or if it varies from test to test.
- The emitters need to have very specific sizes and locations due to the sensitivity of CE to geometry effects. For development purposes, testing was carried out on front heating elements, back heating elements, and a combination of the two. Two heating elements were tested at all times, to allow for any potential plume interactions between parallel plumes above the cooktop.
- The air flows through the range hood are controlled to be the rated range hood flows. This test method is not attempting to address installation issues in kitchens (often measured air flows are less than manufacturer's claimed nominal flows), so the test apparatus includes and flow meter and auxiliary fan to ensure that testing is performed at rated flows. One alternative was considered: using exhaust ducting with standardized air flow resistance that would reflect any performance changes due to installation effects .However, this was thought to add the potential for additional variability between different testing laboratories.

CAPTURE EFFICIENCY TEST METHOD DESCRIPTION

The test method describes a laboratory test apparatus and testing procedure used to develop the ASTM test method for CE based on standardized room, cooking burners and tracer gas emitters, using CO_2 as a tracer gas.

The test chamber floor had a rectangular floor plan 4.6 m (15 ft) by 2.3 m (7.5 ft). The ceiling height was 2.45 m (8 ft) wall height, resulting in a chamber volume of 25.5 m^3 (900 ft^3). In the new ASTM standard, these are minimum test chamber dimensions and a larger test chamber may be used. The European standard for range hood performance (IEC 2005) specifies an exact size of test chamber; however, the ASTM working group wanted users to have some flexibility to allow for use/adaptation of exiting test chambers or in contruction of new test chambers. In this study and the development of the ASTM test method only one size test

chamber was used. Although we measured the tracer gas concentrations in many room locations to ensure that the tracer gas sampling point is representative of the room (Walker et al. (2016)) we have not performed any tests in other test chambers. In the future further testing of the influence of test chamber size and shape would be highly valuable.

The tracer gas concentrations are measured in three locations: inside the test chamber (C_c); at the test chamber inlet (C_i); and in the exhaust ducting (C_e). The concentrations are averaged for a period of 10 minutes after reaching steady state to minimize the effect of the temporal variability in the tracer gas concentration.

The CE is calculated using Equation 2:

$$CE = \frac{C_e - C_c}{C_e - C_i} \qquad (2)$$

Equation 2 is based on an assumption of steady-state concentrations. The analysis represented by Equation 2 has distinct advantages in removing measurement-related biases by using the ratios of differences between two concentrations (C_e-C_c, C_e- C_i). Any calibration coefficient error multiplies both the numerator and denominator, and zero offsets cancel in the subtraction. Note that these advantages are primarily true if the same instrument is used for all three measurements. In practice we did not use the same instrument to achieve these uncertainty reductions due to the sampling delays introduced by the use of sampling manifolds required if only one instrument was used. By using more than one instrument we had more data available for each ten-minute averaged concentration. Other testers may wish to investigate these trade-offs and come to their own decisions, depending on how reliable their test instrument calibrations are and the time available for testing. For example, if calibrations are less reliable and more time is available for testing, then it may be preferable to use a single instrument with a longer averaging time to take advantage of the uncertainty reductions due to the functional form of Equation 2. To minimize the experimental uncertainties when using three separate instruments, daily calibration checks were done with pre-mixed bags of air and tracer over the measurement range used in the testing (known concentrations of 2,466 parts per million [ppm], 1,726 ppm, and 986 ppm).

To identify when the test has achieved steady state, the number of test chamber air changes (n) is used as a metric. The minimum time to reach steady-state conditions is calculated using Equation 3:

$$t = \frac{n * V_{Chamber}}{Q_{air}} \qquad (3)$$

Where
t = minimum time to reach steady state condition
n = number of air changes
$V_{chamber}$ = volume of testing chamber
Q_{air} = air flow rate

To determine the appropriate number of air changes required to reach steady-state conditions, we took tracer gas samples over extended periods of time (up to one hour) and calculated the CE every 10 minutes. Steady state was assumed to be reached when the difference between the consecutive CE values was less than 5%. In most cases, four chamber-air changes were required. In some cases up to eight chamber-air changes were necessary to reach steady-state conditions. A detailed analysis of the time series concentration data indicated that these longer times were due to temporal variations in tracer gas concentrations separate from the gradual approach to steady-state conditions. These temporal variations will be discussed further when we consider test repeatability issues.

TRACER GAS SAMPLING AND TESTING CHAMBER

Carbon dioxide was chosen as a tracer gas for sustainability, safety, and because CO_2 measurement equipment is readily available and of reasonable cost (both of which are factors to consider for a standardized test method that is intended for use in multiple testing laboratories and manufacturers facilities).

Figure 2 and Figure 3 show a schematic of the tracer gas and air flow control apparatus, the cabinetry used in the test chamber, and the tracer gas measurement locations.

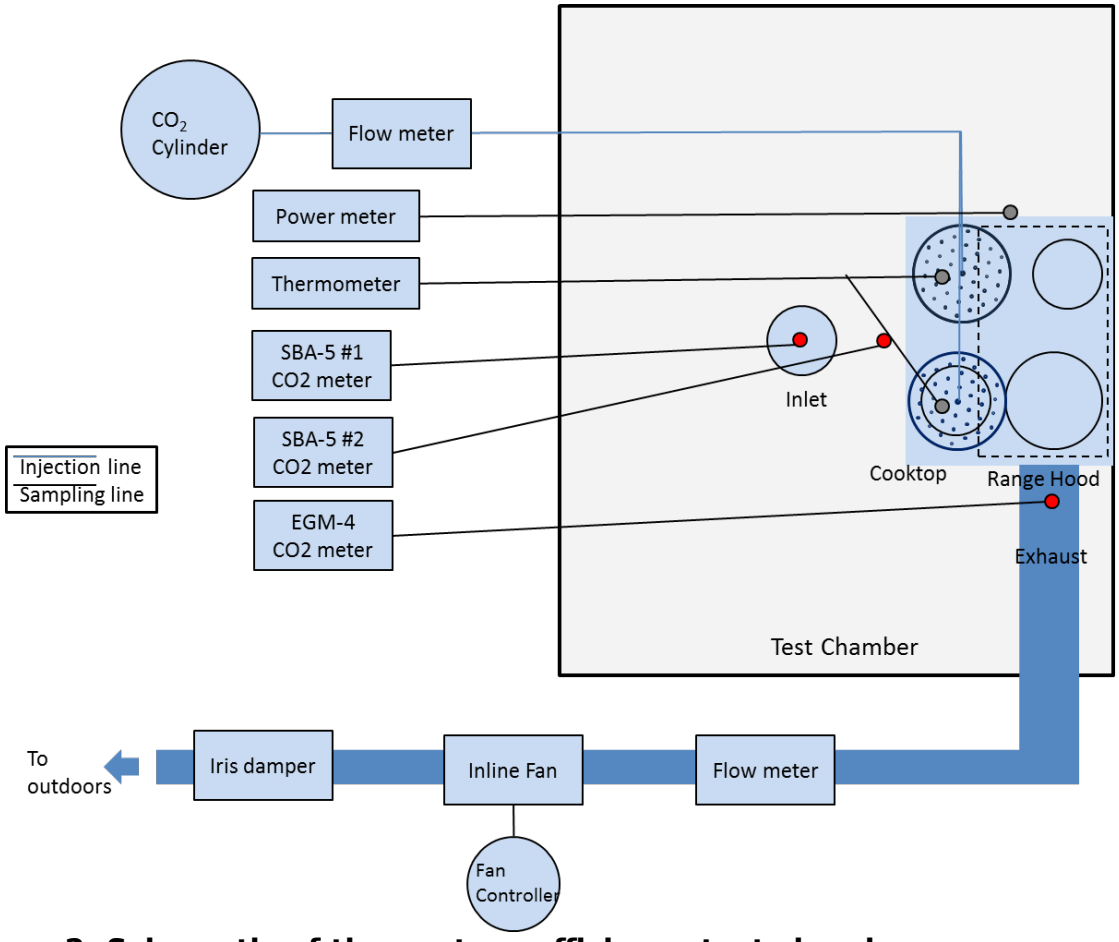

Figure 2. Schematic of the capture efficiency test chamber

Since CO_2 is used as a tracer gas and it is at relatively high concentrations in ambient air (compared to other potential tracer gases), the concentration of CO_2 in the air entering the chamber must be measured. To minimize uncertainties, as much of the air as possible should enter through a known location where its concentration can be measured. Therefore, it is necessary to seal the test chamber to ensure that most of the air that comes to the chamber to make up for the range hood exhaust comes through a known inlet where the concentration of tracer gas is measured (C_i).. In preliminary testing we measured the exhaust tracer gas concentration (C_e) in the exhaust ducting using multiple sample points at different locations in the exhaust duct. The results showed hat that the CO_2 in the exhaust was well mixed, so multiple sample points in the exhaust are not necessary. The room tracer gas concentration (C_c) was measured on the cooktop centerline, 0.5 m (20 in.) into the room from the cooktop, and vertically halfway between the cooktop and the bottom of the range hood. This location was selected based on previous LBNL testing, which measured the tracer gas concentrations at multiple points in the test chamber to determine the representative location of the tracer gas concentration in the air entering the plume (Walker et al. 2016).

The CO_2 concentrations were measured using PP Systems SBA-5 analyzers and an EGM-4 analyzer that have an accuracy of ±1% (±25 ppm) of the calibrated range. The tracer gas injection rate was adjusted depending on the air flow through the range hood such that the steady-state concentration in the exhaust duct was about 2,000 ppm (about 1,500 ppm above ambient). This was selected to be in the center of the range for the CO_2 monitoring equipment. The CO_2 injection flow rate was controlled by a mass flow controller with an accuracy of ±1%. The required tracer gas flows were between 0.15 and 0.3 L/s, or about 0.2% of the total system air flow through the range hood.

A flow meter, iris damper, and auxiliary fan in the exhaust duct were used to measure and control the air flow for the testing range hood, with an accuracy of ±2.5 L/s (5.3 cfm). Although the air flow measurement is not used for CE calculations, it is important to know the air flow for test repeatabilty and consistency. It is likely that any agency referring to the test method will want to specify the test air flow in some consistent way. This could be CE at a given flow rate or at a rated flow, such as those provided by the Home Ventilating Institute (HVI 2015).

Figure 3 shows a schematic of the cabinetry used in the test chamber, locations of the air inlet and exhaust from the test chamber, and the tracer gas sampling locations. The location and geometry of the kitchen cabinetry is specified for consistency of testing because the cabinetry changes flow patterns in the room, and the cabinets to either side of the range hood directly influence flow patterns above the cooktop. The cabinet dimensions were chosen to represent typical kitchen cabinetry.

The test chamber was sealed to a tightness of 2.5 air changes per hour (19 L/s or 37.5 cfm) at 50 Pa (0.2 in. water) to make sure most of the air entering the chamber came from the air inlet. The air leakage test was done by sealing the inlets and outlets and pressurizing the chamber to 50 Pa. At typical pressure differences

induced during testing, roughly 1.5 to 2.5 L/s (3 to 5 cfm) will enter the chamber via this background leakage. This is about 1.5% of the total air flow entering the testing chamber. The diameter of the air inlet was 25.4 cm (10 in.).

The cooktop was located in the center of the long wall of the chamber. Figure 4 shows the schematic of heating elements on the cooktop and the actual cooktop used in this test. The size of cooktop was 76 cm (30 in.) wide, 65 cm (25.5 in.) deep, and 90 cm (35.4 in.) tall. The cooktop has two 14 cm (5.5 in.) diameter heating elements with 1,250 W power capacity and two 17 cm (6.7 in.) diameter heating elements with 2,100 W power capacity. The input power for the heating elements was monitored using an ELITEpro XC™ Energy Logger with an accuracy of ±0.2%.

Figure 4. Schematic of the heating elements on the cooktop

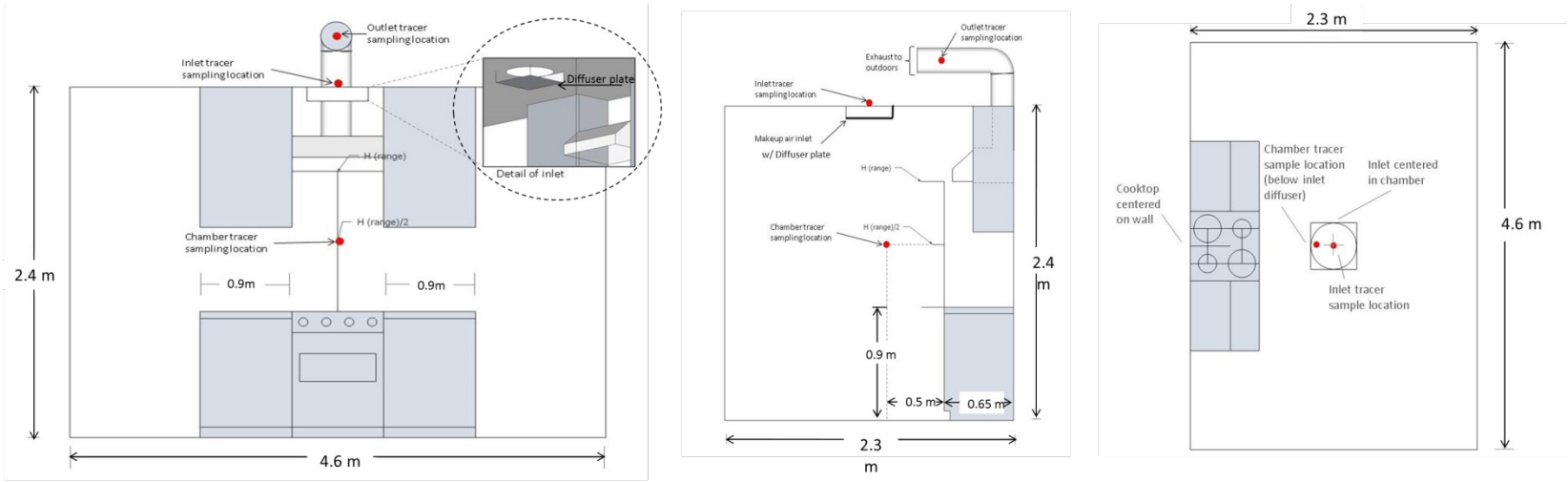

Figure 3. Schematic of the capture efficiency test chamber

The testing method procedure is as follows:

a. The range hood is installed according to the manufacturer's instructions and the distance between the bottom of the range hood and the cooktop recorded.
b. The location of the test chamber tracer gas measurement is adjusted depending on the mounting height of the range hood.
c. The range hood is turned on and set to the desired operating speed. If necessary the auxiliary fan is used to achieve the required air flow.
d. The heating elements are turned on and adjusted to maintain a power input of 1,000 W. The actual power input and tracer gas emitter surface temperatures are recorded.
e. The tracer gas flow is adjusted to achieve a concentration in the range hood exhaust that gives a sufficient signal to be far from any background concentration but with instrumentation limits.
f. Once the system reaches steady state by waiting for the difference between the consecutive time averages was less than 5% to complete, record at least 10 minutes of data.
g. CE is calculated using Equation 2.

RESOLVING TRACER GAS EMITTER AND TEST CHAMBER AIR INLET ISSUES

An important aspect of standardized testing is repeatability of results. To examine this we performed tests where CE was measured several times for the same range hood with the same mounting height, air flow, and heating element configuration. The tracer gas sampling was performed for up to an hour after reaching steady state, which allowed us to calculate several 10-minute average samples. We calculated the mean and standard deviation over these multiple tests (typically four or five replications). For some tests the standard deviation in CE was small: 0.3% to 0.6%. However, some tests had a greater standard deviation of 1.6% to 1.7%, and one configuration was as high as 2.5%—with greater variability at higher air flows. We considered this level of repeatability uncertainty to be too high. Further investigation of the time series data allowed us to observe that this variability was not simply due to noisy signals (that could be treated with longer time averaging, for example) but to relatively long-term systematic concentration changes/cycles on the order of several minutes in duration. Therefore, we tried to identify possible causes for these fluctuations and make changes to the testing to reduce them. We focused on two features we assumed were causing problems: (1) design issues with the tracer gas emitters, and (2) fluctuations of the air movement in the chamber.

Tracer gas emitter development

The tracer gas emitters have two functions:

1. To uniformly seed the hot plume with tracer gas.
2. To create a thermal and geometric equivalent to a typical cooking event.

Both functions need to be achieved in a highly replicable way.

Figure 5 (a) shows the tracer gas emitters from the initial test method (Walker et al. 2017) that were used in the repeatability testing discussed above. The emitter assembly had four parts: a 28 cm (11 in.) diameter heat diffusion plate, a 23 cm (9 in.) diameter pan, a spacer to separate the heat diffusion plate from the pan, and perforated copper coils for tracer gas emission. This configuration was developed based on some readily available components. The spacer was chosen so we could maintain the desired 200°C (390°F) upper surface temperature with a 1,000 W power input. The perforated copper coils were connected to the tracer gas controller to inject the tracer gas through small holes in the copper tubing. This approach had several issues:

- It effectively seeded the plume above the pans, but it did not effectively seed the plume from the heating elements.
- It proved to be difficult to uniformly seat the perforated copper coils in the pan, making replication questionable between tests.
- The assembly of plates, spacer, and pan would be difficult to replicate exactly in another laboratory, and therefore did not lend itself to a standardized test method.

To address these issues, new tracer gas emitters were developed using machined plates that can be accurately reproduced, and that inject the tracer gas over the whole plume to include both the plume directly from the top of the pan and the plume coming from the heating elements around the sides of the pot or pan. Figure 5(b) is a photograph of these new tracer gas emitters on the cooktop and Figure 5(c) is a schematic of the tracer gas emitter assemblies. The new emitters are machined aluminum plates of 25.4 cm (10 in.) diameter. Three main parts are required to assemble the tracer gas emitter: an upper plate with 36 holes evenly distributed over its surface, a tracer gas plenum that is machined into a second plate that also emits tracer gas through 18 holes on its lower face, and a third (solid) heat diffusion plate. The first and second plate are sandwiched together to form a single upper injector plate. The upper plate has holes to emit tracer gas on the upper surface, between the injector plate and the bottom plate so that the entire plume is seeded. A set of 12.7 mm (0.5 in.) ceramic standoffs were used to separate the upper injector plate from the solid bottom plate. This allowed for the emitter plates to have the correct target power input (1,000 W/plate) while maintaining an upper surface temperature of 200°C (390°F). More details on the emitted plate development are provided in Kim et al. 2017.

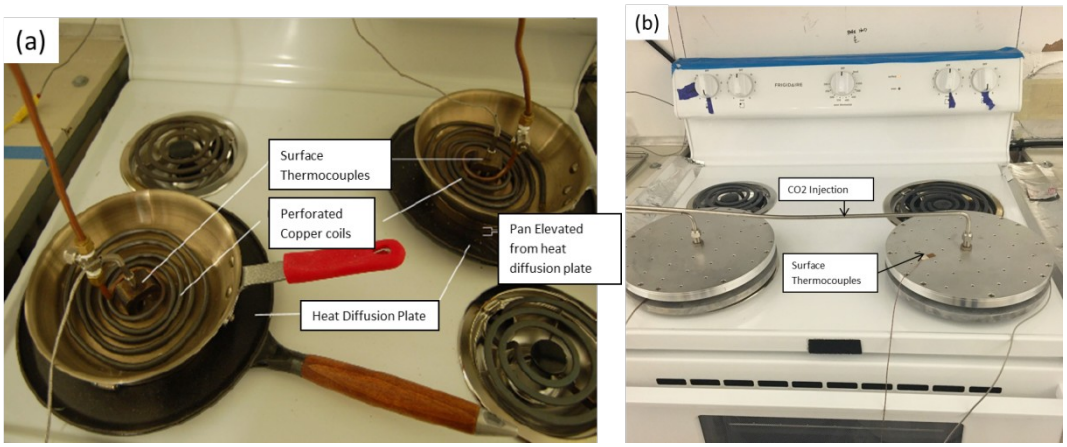

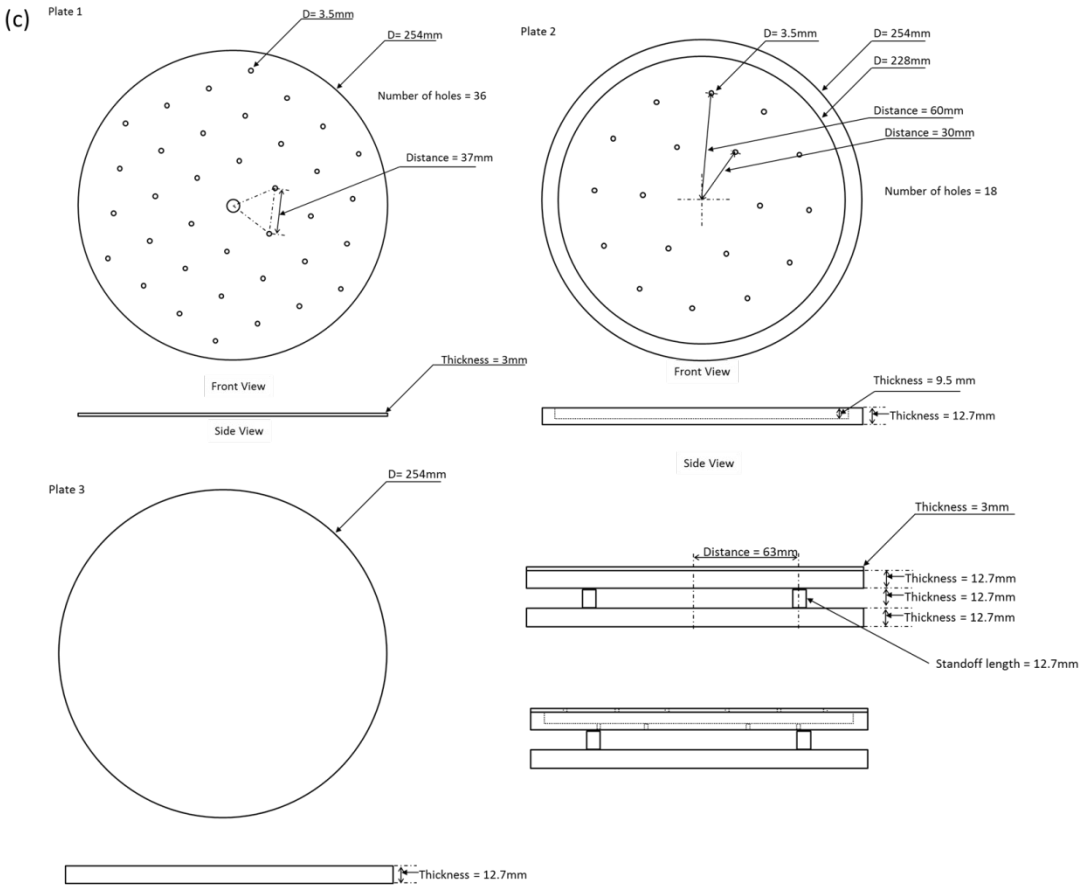

Figure 5. Tracer gas emitters (a) old emitters, (b) new emitters, and (c) schematic of the tracer gas emitters

In actual cooking activities, Kosonen et al. (2006b) showed that during frying, the energy removed by convection is only around 6%–20% of total energy input, and more than 50% of energy was dissipated via radiation. For the emitter plates developed for this test method, and assuming $T_{surface}$ = 200°C of top plate, T_{room} = 25°C, 0.3 L/s tracer gas injection at very low temperature T_{tracer} = 0°C, Figure 6 shows how input energy is transferred to environment and the plume. The convective heat transfer to the plume (q_{conv}) was estimated from standardized heat transfer relationships for heat transfer coefficients (Bergman et al. 2011) for heated plates facing upward: $q_{conv}=hAdT$. The conductive heat transfer (q_{cond}) was estimated using $q_{cond}=UAdT$. The radiation heat transfer was estimated using an assumed surface emissivity of 0.3, $q_{rad}=\epsilon\sigma T^4$. Where: A= surface area (m^2) , T = temperature (K), dT = temperature differences (K) , h = convective heat transfer coefficient (W/m^2K) , σ = Stefan-Boltzmann number (W/m^2K^4) , ϵ= emissivity and U = coefficient of heat transfer. We estimate that roughly 10% of the energy is used to heat the tracer gas, and about 15% of the energy is removed via convection from the top plate and radiation at the top plate, which is driven by the surface temperature. Roughly 20% of energy is moving from the space between the top plate and the bottom plate by convection and radiation. The remaining energy is removed by the forced convection air flows due to range hood operation and by radiation from the hot bottom plate (that reaches temperatures up to 500°C – note

that at these elevated temperatures it may be a good idea to use steel rather than aluminum to construct the emitter) to the environment.

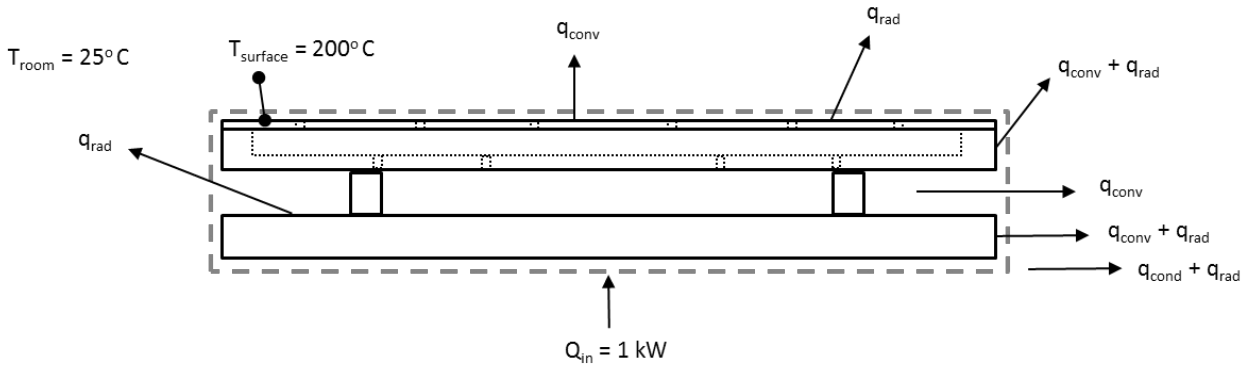

Figure 6. Heat transfer from new emitters

To evaluate the new tracer gas emitters, tests were performed for three different heating element configurations (front, back, and one each front and back) with two different types of range hoods and two different mounting heights for each range hood, for a total of 12 tests. For all configurations, the range hoods showed higher capture efficiency when using the new emitters. The changes are greater for the low CE cases, with more than a 10% increase in CE. This is a somewhat surprising result, we would expect that seeding more of the plume edges (as the new emitters do) might lead to less indicated capture because it is the edges of the plume that we expect to be captured less efficiently. It is possible that this result is because of the change in physical geometry of the emitters, however, this remains a topic for future investigation. This result also shows that the CE results are definitely sensitive to the emitter design and reinforces that need to use a replicable emitter for standardized testing.

Air Flow Patterns in the Test Chamber and Chamber Air Inlet Design

The second parameter suspected of causing the variability from test to test was air flow patterns in the test chamber because the greatest variability was at the highest tested air flow. At high air flow, make-up air from the air inlet produced a high velocity air jet that could change the air flow patterns in the room and therefore CE (Zhang et al. 1990; Fritz 1989; Clark 2009). To investigate this effect, tests were performed using additional tracer gas sampling locations in the test chamber. These additional sample locations were above, below, and to either side of the single reference point, with one sample from under the upper cabinets to the right of the range hood. In addition to comparing the tracer gas concentrations at each location, we calculated the CE based on these measured room concentrations.

We observed that the tracer gas concentrations at each location rose and fell together, resulting in similar measured concentrations (within about 40 ppm of the reference [roughly a 5% change in the concentration differences used in the CE calculation]) and similar changes in CE for almost all locations. The exception was the one sample under the cabinets that showed much greater fluctuations and was about 200 ppm (20% of room tracer gas concentration) higher than other locations. These systematic changes indicated that specific flow patterns might be set up in the test chamber due to the air flow velocities from the air inlet into the test

chamber. More details of these systematic temporal variations can be found in Kim et al. (2017).

Figure 7 (a) shows the detail of the original air inlet. A 30.5 cm x 30.5 cm (12 in. x 12 in.) deflection plate was located 4.5 cm (1.8 in.) below the ceiling to prevent inlet air from blowing directly on the range hood and cooktop. The deflector plate was blocked on the side that faced the cooktop/range hood and was open on the other three sides. We made air velocity measurements near the air inlet using velocity probes (TA-5 Thermal Anemometer with an accuracy of ±2% of range). We measured air velocities of 3 meters per second (m/s) (592 feet per minute [fpm]) at the diffuser plate and 1 m/s (197 fpm) at the ceiling at an 80 L/s (161 CFM) exhaust flow. We redesigned the air inlet in an attempt to reduce these velocities and the variability in measured CE.

Figure 7 (b) shows the new air inlet box. Like the first inlet it has a closed bottom and side facing the cooktop/range hood, to prevent direct air flow in toward the range hood and cooktop. A circular diffuser was installed in the inlet opening in the ceiling, and a diffuser box, made from MERV 11 filters with sides 30 cm (12 in.) long, was installed to ensure that the air would enter the room at a lower velocity and more uniformly. With the same exhaust flow (80 L/s [161 CFM]) and a new air inlet, the average air velocities were reduced to 0.7 m/s at 10 cm away from the filter and were uniform over the diffuser box outlet area (ranging from 0.6 to 0.75 m/s). More details of these measurements are given in Kim et al. (2017). The new air inlet box made the room concentrations uniform —in particular the large variability to the side of the range hood was eliminated. The key issue is that low inlet velocities should be used in the testing to prevent setting up unstable flow patterns. Our inlet box is just one example of how to achieve this. Other methods using large area diffusers to keep inlet velocities low would also be acceptable. For example, Fritz (1989) suggested the perforated plate type design to avoid the creation of an air curtain, which is caused by the direct airflow from the make-up air diffuser.

Figure 7. Detail of air inlet: (a) old version; (b) new version (with a ceiling diffuser and MERV 11 air filters)

For comparison to the old inlet tests, the same combination of 12 tests were repeated with the new inlet. The new inlet reduced the standard deviation of the tests to the 0.3% to 0.9% range with one exception: the test with greatest variability was reduced from 2.5% to 1.4% standard deviation. Although imperfect, these results are a significant improvement.

RESULTS

To determine if the initial test method produced reasonable results that could be used to develop a standard test method, 27 trial tests were conducted with the initial test method on eight different range hoods (Walker et al. 2016). Table 1 shows the summary of the eight tested range hoods.

Table 1. Summary of Range Hood Characteristics

Range Hood	Depth from wall cm (in.)	Geometry
A	48 (19)	Deep sump with grease screen on one central intake
B	53 (21)	Deep sump, no grease screen central intake
C	48 (19)	Flat with grease screens—2 intakes at left and right edges
D	46 (18)	Flat with 2 large grease screens covering 70% of underside
E	56 (22)	Shallow sump, no grease screen—intake over entire underside
F	38 (15)	Flat with 2 small grease screens at extreme left and right
G	64 (25)	Shallow sump, no grease screen—2 intakes centered in each half
H	46 (18)	Flat with grease screen on one central intake

Figure 8 shows results from the tests conducted with the initial test method: the original air inlet, original tracer gas emitters (one at the back and one near the front), and different mounting heights (the larger symbols are for the higher mounting level and the smaller symbols for the lower mounting level).

The tests showed that generally, capture efficiency increases with higher airflow and lower mounting height. Also, capture efficiencies across different configurations and models varied considerably for a given air flow. For instance, the measured capture efficiency for the tests at 75 L/s (150 cfm) ranged from 65%–90%. As with the results shown in Figure 1 from previous studies, the variation suggests that range hood geometry and mounting height significantly impact the CE of range hoods.

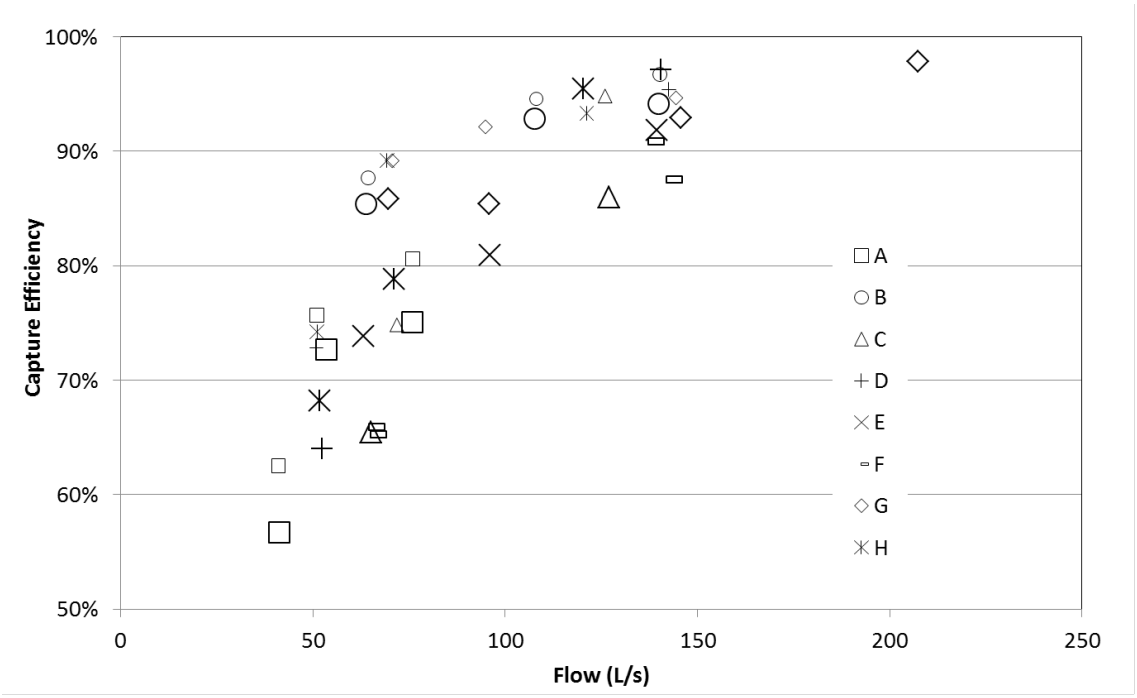

Figure 8. Capture efficiency versus airflow for the eight range hood models tested for the initial test method (larger symbols for the higher mounting level and the smaller symbols for the lower mounting level)

Figure 9 and Table 2 show results from the tests conducted with the final test method, which features the new emitters and new air inlet (for more details, see Kim et al. (2017)). The figure shows two different heating element/emitter position configurations (open symbols for one at the back and one near the front, and filled symbols for two fronts) and different mounting heights (larger symbols for the higher mounting level (A: 61 cm, B: 69 cm) and the smaller symbols for the lower mounting level (A: 46 cm. B 61 cm)). These results are for the same two range hoods (A and B) used in earlier testing (Figure 8) . As expected, the CE was higher when a high airflow was used, and CE was higher with lower mounting height, except for range hood B using the one front and one back emitter configuration. For the same mounting height and air flow, CE was lower for the two front-emitter configurations compared to the one front and one back emitter configuration. In addition, the range of results is greater for the configuration with two front emitters (63%–95% CE) compared to one front and one back (74%–99% CE). The generally lower CE and higher CE variability for front emitters is similar to the previous study results (Delp and Singer 2012) and is due to geometry effects—the hoods do not cover the front burners, and it is therefore harder to capture the plume. This higher sensitivity when using two front heating elements allows greater resolution of differences in range hood performance and is the approach that has been recommended for the ASTM test method.

Table 2. Capture efficiency results for the two range hood models with changes of the emitters' position

Model	Mounting Height (cm)	Airflow (L/s)	Two Front Emitters	Front and Back Emitters
A	46	75	89% (±0.5%)	95% (±0.4%)
A	61	75	87% (±0.3%)	92% (±0.4%)
A	46	50	65% (±0.9%)	78% (±0.8%)
A	61	50	63% (±0.7%)	74% (±0.7%)
B	61	129	95% (±1.4%)	99% (±0.3%)
B	69	129	91% (±0.9%)	99% (±0.5%)

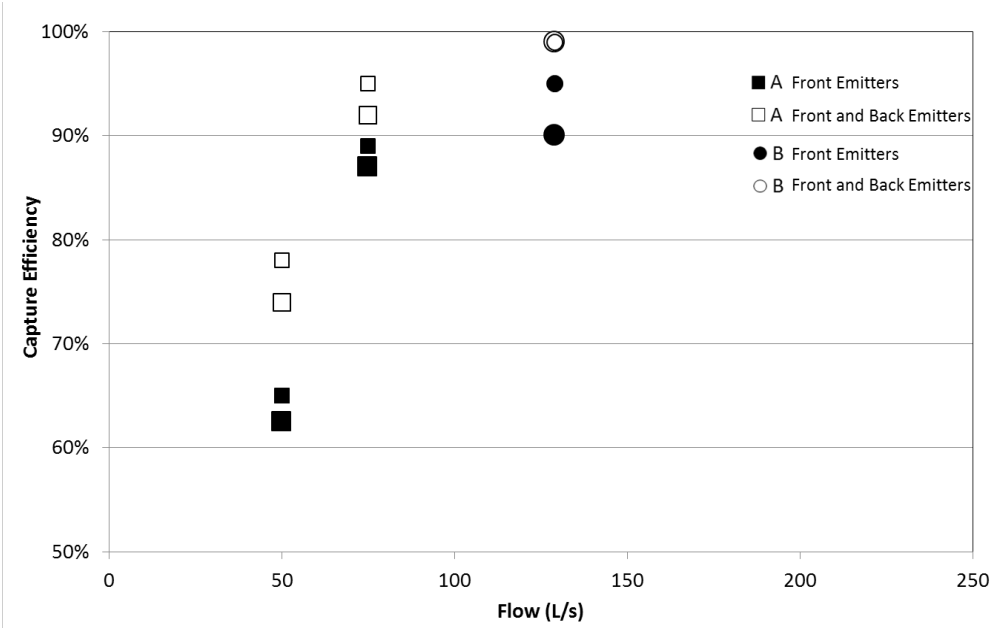

Figure 9. Capture efficiency versus airflow for the two range hood models tested for the new test method (larger symbols for the higher mounting level and the smaller symbols for the lower mounting level)

SUMMARY

This paper discusses the development of a standardized test procedure for evaluating residential wall-mount range hood capture efficiency. Initial range hood test method development at LBNL (Walker et al. 2017) identified parameters that need to be controlled for standardized testing.

- Fixed installation geometry. This includes test chamber, kitchen cabinetry, and cooktop dimensions, and locations for tracer gas sampling.
- Use of a tracer gas technique to measure CE.
- Fixing power and temperature requirements for heating elements

Additional experiments described in this paper led to test refinements: use of a single specific tracer gas emitter design, the use of two front heating elements, and limiting air inlet velocities to the test chamber.

Using two front heating elements, the new diffuse air inlet, and 10-minute averaging, and waiting four chamber-air changes for steady state resulted in repeatability uncertainties typically ±0.5% CE, with ±1.4% CE at worst.

The next steps to be taken in standardized testing of kitchen range hoods are to develop test procedures for island and downdraft hoods and to include larger cooktops with more heating elements.

REFERENCES

ASHRAE. 2016 Standard 62.2 Ventilation and Acceptable Indoor Air Quality inResidential Buildings. ASHRAE, Atlanta, Georgia.

ASTM. 2009. F1704-09. Standard Test Method for Capture and Contaminant Performance of Commercial Kitchen Exhaust Ventilation Systems. American Society of Testing and Materials.

Buonanno, G., L. Morawska, and L. Stabile. 2009. “Particle Emission Factors During Cooking Activities.” *Atmos. Environ.* 43(20): 3235–3242.

Bergman, T.L., A. S. Lavine, F. P. Incropera, and D. P. DeWitt. 2011. *Fundamentals of Heat and Mass Transfer* 7th ed. Wiley.

Clark, J. A. 2009. “Solving Kitchen Ventilation Problems.” *ASHRAE Journal.* 51 (7):20–24.

Delp, W. W., and B. C. Singer. 2012. “Performance Assessment of U.S. Residential Cooking Exhaust Hoods.” *Environ. Sci. Technol*. 46(11): 6167–6173.

Dennekamp, M., S. Howarth, C. A. J. Dick, J. W. Cherrie, K. Donaldson, and A. Seaton. 2001. “Ultrafine particles and nitrogen oxides generated by gas and electric cooking.” *Occupational and Environmental Medicine* 58(8): 511–516.

Fritz, R. L. 1989. “A Realistic Evaluation of Kitchen Ventilation Hood Designs.” *ASHRAE Transactions*. 95(1): 769–779.

Farnsworth, C., A. Waters, R. M. Kelso, and D. Fritzsche. 1989. “Development of a Fully Vented Gas Range.” *ASHRAE Transactions,* 95(1): 759–768.

Gao, J., C. Cao, Q. Xiao, B. Xu, X. Zhou, and X. Zhang. 2013. “Determination of dynamic intake fraction of cooking-generated particles in the kitchen.” *Building and Environment*. 65: 146–153.

He, C., L. Morawska, J. Hitchins, and D. Gilbert. 2004. “Contribution from Indoor Sources to Particle Number and Mass Concentrations in Residential Houses.” *Atmos. Environ.* 38(21): 3405–3415.

HVI. 2015. Certified Home Ventilating Products Directory. Home Ventilating Institute publication 911. HVI, Morehead City, North Carolina.

Honda, Y., H. Kotani, Y. Toshio, S. Kazunobu, and Y. Momoi. 2012. Modeling the thermal plume around cooking pot for prediction of thermal plume above residential gas cooking stove. Proceedings of the 5th international building physics conference, pp. 1083–1091.

Huang, Y., S. S. H. Ho, K. F. Ho, S. C. Lee, J. Z. Yu, and P. K. Louie, 2011. Characteristics and health impacts of VOCs and carbonyls associated with residential cooking activities in Hong Kong. *Journal of hazardous materials*, 186(1): 344-351.

IEC. 2005. International Standard IEC 61591. Household range hoods–methods for measuring performance. CEI/IEC 61591:1997+A1.

Kim, Y-S, I. S. Walker, and W. W. Delp. 2017. "Development of a Standard Test Method for Reducing the Uncertainties in Measuring the Capture Efficiency of Range Hoods." LBNL Report 2001009.

Kosonen, R., H. Koskela, and P. Saarinen. 2006a. "Thermal Plumes of kitchen appliances: Idle mode." *Energy and Buildings* 38(9): 1130–1139.

Kosonen, R., H. Koskela, and P. Saarinen. 2006b. "Thermal Plumes of kitchen appliances: Cooking mode." *Energy and Buildings* 38(9): 1141–1148.

Kuehn, T. H., J. Ramsey, H. Han, M. Perkovich, and S. Youssef. 1989. "A Study of Kitchen Range Exhaust Systems." *ASHRAE Transactions*, 95(1): 744–752.

Li, Y. and A. Delsante. 1996. "Derivation of Capture Efficiency of Kitchen Range Hoods in a Confined Space." *Building and Environment* 31(5): 461–468.

Lunden, M. M., W. W. Delp, and B. C. Singer. 2015. "Capture efficiency of cooking-related fine and ultrafine particles by residental exhaust hoods." *Indoor Air* 25:45–58.

Logue, J. M., N. E. Klepeis, A. B. Lobscheid, and B. C. Singer. 2013. "Pollutant Exposures from Natural Gas Cooking Burners: A Simulation-Based Assessment for Southern California." *Environ. Health Perspect.* 122(1):43–50.

Monserrat, L. 2016. OEHHA Acute, 8-hour and Chronic Reference Exposure Level (REL) Summary. OEHHA.

Rim, D., L. Wallace, S. Nabinger, and A. Persily. 2012. "Reduction of Exposure to Ultrafine Particles by Kitchen Exhaust Hoods: The Effects of Exhaust Flow Rates, Particle Size, and Burner Position." *Sci. Total Environ.* 432: 350–356.

See, S. W., S. Karthikeyan, and R. Balasubramanian, 2006. "Health risk assessment of occupational exposure to particulate-phase polycyclic aromatic hydrocarbons associated with Chinese, Malay and Indian cooking." *J. Environ. Monit.*, 8(3): 369-376.

Siegmann, K., and K. Sattler. 1996. "Aerosol from hot cooking oil, a possible health hazard." *J. Aerosol Sci.* 27:S493-S494.

Singer, B. C., W. W. Delp, and M. G. Apte. 2010. *Experimental Evaluation of Installed Cooking Exhaust Fan Performance.* LBNL-4813E.

Singer, B. C., W. W. Delp, P. N. Price, and M. G. Apte. 2012. "Performance of Installed Cooking Exhaust Devices." *Indoor Air* 22(3):223–234.

U.S. Environmental Protection Agency, NAAQS Table.

Walker, I. S., J. C. Stratton, W. W. Delp, and M. H. Sherman. 2016. "Development of a Tracer Gas Capture Efficiency Test Method for Residential Kitchen Ventilation". LBNL-1004365.

Walker, I. S., M. H. Sherman, and B. C. Singer. 2017. "Development of a Tracer Gas Capture Efficiency Test Method for Residential Kitchen Ventilation." *American*

Society of Heating, Refrigerating and Air-Conditioning Engineers 2016 IAQ-39mslRK.

Wallace, L. A., W. R. Ott, C. J. Weschler, and A.C. Lai. 2017. “Desorption of SVOCs from heated surfaces in the form of ultrafine particles.” *Environ. Sci. Technol.*, 51(3): 1140-1146.

Wallace, L. A., W. R. Ott, and C. J. Weschler. 2015. “Ultrafine particles from electric appliances and cooking pans: experiments suggesting desorption/nucleation of sorbed organics as the primary source.” *Indoor Air* 25(5): 536-546.

Zhang, J. S., L. L. Christianson, and G. L. Riskowski. 1990. “Regional Airflow Characteristics in a Mechanically Ventilated Room Under Nonisothermal Conditions.” *ASHRAE Transactions* 96(1): 751–759.

Zhang, Q., R. H. Gangupomu, D. Ramirez, and Y. Zhu. 2010. “Measurement of Ultrafine Particles and Other Air Pollutants Emitted by Cooking Activities.” *Int. J. Environ. Res. Public. Health* 7(4):1744–1759.